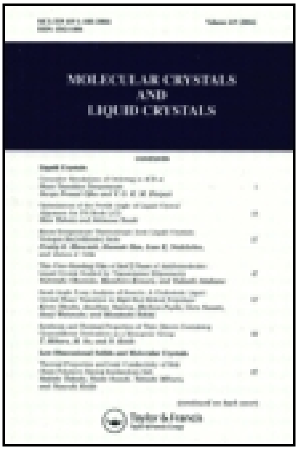

Molecular Crystals and Liquid Crystals Science and Technology. Section A. Molecular Crystals and Liquid Crystals

Publication details, including instructions for authors and subscription information:
http://www.tandfonline.com/loi/gmcl19

Asymmetric Tilt and Twist Coupling for Chiral-Nematic Layers

W. L. Wagner [a] [b]

[a] Forschungsgruppe Flüssigkristalle, 10117, Berlin, FRG

[b] Technische Universität Berlin Sekr, PN7-1, Hardenbergstr. 36, D-10623, Berlin

Version of record first published: 23 Sep 2006.

Mol. Cryst. Liq. Cryst., 1994, Vol. 257, pp. 113–124
Reprints available directly from the publisher
Photocopying permitted by license only

Asymmetric Tilt and Twist Coupling for Chiral-Nematic Layers

W. L. WAGNER[†]

Forschungsgruppe Flüssigkristalle, 10117 Berlin, FRG

(Received July 22, 1993; in final form January 7, 1994)

The influence of an asymmetrical boundary coupling on the field-induced director patterns in chiral-nematic layers is investigated. Weak anchoring is assumed for the tilt coupling as well as for the twist coupling. For different tilt coupling conditions at the boundaries the symmetry of the director patterns breaks down. In contrast, an asymmetric twist coupling does not influence the symmetry of the director patterns. The assumption of the weak twist coupling at one boundary surface only is sufficient to discuss all cases of interest without loss of generality.

INTRODUCTION

A lot of theoretical and experimental work has been published dealing with the director deformations of twisted nematic layers under external fields.[1,2,3] From an applicational point of view the calculation of the director patterns is the first step in the prediction of the electro-optical properties[4,5,6] of liquid crystal (LC) devices. The director configuration is the result of the interplay between elastic forces, external field and surface interactions. Depending on the application purpose particular boundary conditions have to be realized in the LC sample. Applying special surface treatments (rubbing, evaporating) it is possible to orient the molecules at the boundaries in a certain direction, as a result of anisotropic interactions between the constituent molecules and the substratum.[7,8] If the boundary orientations do not change under the influence of external forces we have the case of strong (rigid) coupling. In the alternative case of weak coupling the equilibrium boundary orientations depend on the applied field. Usually, the anchoring conditions at both sides of the liquid crystal layer are assumed to be equal to each other (symmetric boundary coupling). In the present paper we investigate the influence of an asymmetric boundary coupling on the director patterns. Weak tilt coupling as well as weak twist coupling are taken into consideration.

Preliminary results have been presented in Reference 9. We shall not deal with the consequences for the optical properties (see e.g., Reference 10).

[†] Present address: Technische Universität Berlin Sekr. PN7-1, Hardenbergstr. 36, D-10623 Berlin.

SYMMETRY

Applying surface alignment techniques preferential orientations can be created at the LC/substratum interface. In the weak anchoring case the coupling conditions are described by tilt and twist and by the coupling constants,[11] which are a measure of the interaction strength at the interface. If the orientational angles and the coupling constants of the corresponding type are equal at both boundaries, we have symmetric coupling conditions. The corresponding tilt profile looks symmetrically with respect to the mid-plane of the layer, and the twist profile exhibits a mirror point at the mid-plane. In that case the problem can be solved in a half-plane. This symmetry breaks down if we allow different coupling conditions at both sides of the LC layer. Different preferential axes as well as different coupling constants are possible. The main consequence is the variable location of the extreme director tilt θ_m in the sample. The position depends on the coupling conditions as well as on the applied voltage. In this situation, a critical voltage for which the director orientation is uniform throughout the sample no longer exists. Instead of this, we find a voltage range with monotonic behaviour of the tilt profile.

GENERAL THEORY

We consider a nematic layer located between the boundary surfaces at $z_1 = 0$ and $z_2 = d$. The orientation of the liquid crystal director is specified by the polar angle $\theta(z)$ (measured from the layer plane) and by the azimuth $\phi(z)$.

The surface treatment produces preferential orientations θ_{pi} (pretilt) and ϕ_{pi} (pretwist) of the molecules at the boundaries. The equilibrium orientations of the molecules at the boundary surfaces θ_i and ϕ_i vary with the applied field. Even for zero voltage the equilibrium orientations are different from the preferential axes because of the weak anchoring. The twist angles at the lower and upper boundary surfaces are measured in opposite directions, so that the effective twist of the layer is given by

$$\phi_0 = \phi_1 + \phi_2 \text{ and the total pretwist is } \phi_p = \phi_{p_1} + \phi_{p_2}.$$

The equilibrium orientations of the director are found by solving the variational problem for the free energy W of the system with respect to θ and ϕ. Contributions from the orientational elasticity, the applied field and the surface coupling are taken into account

$$W = W_{elast} - W_{el} + \Sigma_i(W_{si} + W_{si}^*).$$

The elastic term contains the Frank[12] elastic constants k_{ii} and a helical contribution t_0, because generally a chiral additive is added to the nematic host to stabilize the external twist of the layer. Because we perform the variation under the condition of fixed voltage, the electric term is taken into account with a minus sign. For the weak coupling with respect to the tilt and twist angle we apply the

Rapini–Papoular model[11,18]

$$W_{si} = \frac{c_i}{2}\sin^2(\theta_i - \theta_{pi}) \tag{1}$$

$$W^*_{si} = \frac{c^*_i}{2}\sin^2(\phi_i - \phi_{pi}) \quad i = 1, 2 \tag{2}$$

where c_i and c^*_i are the coupling constants for the tilt and twist coupling, respectively.

The electric field is applied in z-direction. Therefore, the symmetry of the problem requires all quantities to be functions of the coordinate z only.

We ignore space-charge and flexoelectric effects. Solving the variational problem we get two coupled differential equations in θ and ϕ for the bulk. We integrate these Euler–Lagrange equations under the assumption of the existence of an extreme director tilt θ_m. The derivative of the local twist at the same position is denoted by β. This procedure is known from the symmetrical case[1,2], where the extreme director tilt is located in the mid-plane always.

After integrating again the resulting differential equations we can establish the Equations (4) and (5). Using the relation between the applied voltage u and the dielectric displacement D_z

$$u = \int_0^d E_z\,dz = \frac{D_z}{\varepsilon_0\varepsilon_2}\int_0^d h(\theta)\,dz \tag{3}$$

we derive Equation (6).

Now we have a system of three coupled equations to determine the unknown quantities θ_m, β and the dielectric diplacement D_z. All other quantities can be derived.

The following material parameters come into play

$$\alpha = (k_{33} - k_{22})/k_{22}, \quad \kappa = (k_{33} - k_{11})/k_{11}$$
$$\gamma = (\varepsilon_2 - \varepsilon_1)/\varepsilon_1$$
$$t_0 = 2\pi/p_0$$

p_0 is the pitch of the helical system.
k_{ii}—elastic constants
$\varepsilon_1, \varepsilon_2$—dielectric constants parallel and perpendicular to the director

$$\sqrt{\eta} = \phi_0 * \left[\int_{s_1}^{s_2} \frac{g_m + t_0^*\beta^{-1}*(e_m - e)}{w^*g^*\sqrt{1-\eta s^2}}\,ds\right]^{-1} \tag{4}$$

$$\beta = \frac{\sqrt{\eta}}{d}\int_{s_1}^{s_2} \frac{ds}{w^*\sqrt{1-\eta s^2}} \tag{5}$$

$$\lambda = \frac{u_0 * \sqrt{\gamma * \eta}}{\pi * u}\sqrt{k_{22}/k_{11}}\int_{s_1}^{s_2} \frac{h^*\,ds}{w^*\sqrt{1-\eta s^2}} \tag{6}$$

where $s=\sin\theta/\sin\theta_m$, $s_1=\sin\theta_1/\sin\theta_m$, $s_2=\sin\theta_2/\sin\theta_m$, $\eta=\sin^2\theta_m$ and $\lambda=(\beta/D_z)^*\sqrt{k_{22}{}^*\varepsilon_0{}^*\varepsilon_1}$,

$$\begin{aligned}
w &= \pm(\sqrt{k_{22}/k_{11}}/\sqrt{f^*g})^*\{g^*g_m+g/\lambda^{2*}(h-h_m)-[g_m+t_0/\beta^*(e_m-e)]^2\}^{1/2}\\
e &= e(\theta)=\sin^2\theta-1\\
f &= f(\theta)=1+\kappa^*\sin^2\theta\\
g &= g(\theta)=\cos^2\theta^*(1+\alpha^*\sin^2\theta)\\
h &= h(\theta)=(1+\gamma\sin^2\theta)^{-1}\\
e_m &= e(\theta_m)\text{ a.s.o.}
\end{aligned}$$

The region of integration has to be interpreted as follows

$$\int_{s_1(z_1=d)}^{s_2(z_2=d)}=\int_{s_1}^{1}-\int_{1}^{s_2}.$$

The minus sign results from the fact that the derivative $d\theta/dz=\beta^*w$ changes its sign at the extremum $\theta=\theta_m$. Note that the derivative possesses different signs for minima and maxima, respectively.

The non-linear bulk equations have the same form as in the case of strong surface coupling (For the consequences see below.). From the variational procedure we get the following equations, describing the surface torque balances

$$\frac{\partial W_{elast}}{\partial\theta^{\prime}}+\frac{\partial W_{s2}}{\partial\theta}=0,\quad z_2=d$$

$$\frac{\partial W_{elast}}{\partial\theta^{\prime}}-\frac{\partial W_{s1}}{\partial\theta}=0,\quad z_1=0\quad\text{where }\theta^{\prime}=d\theta/dz.$$

Corresponding equations hold for the twist coupling

$$\frac{\partial W_{elast}}{\partial\phi^{\prime}}+\frac{\partial W^*_{s2}}{\partial\phi}=0,\quad z_2=d$$

$$\frac{\partial W_{elast}}{\partial\phi^{\prime}}-\frac{\partial W^*_{s1}}{\partial\phi}=0,\quad z_1=0\quad\text{where }\phi^{\prime}=d\phi/dz.$$

Inserting the Rapini–Papoular ansatz for the surface potential we arrive, after some rearrangements, at the equations

$$\sin 2(\theta_1-\theta_{p1})=\frac{2}{\pi}r_1*f(\theta_1)*w(\theta_1)\tag{7}$$

$$\sin 2(\theta_2-\theta_{p2})=\frac{2}{\pi}r*f(\theta_2)*w(\theta_2)\tag{8}$$

$$r_i=\pi*k_{11}/(c_i*d)$$

for the tilt coupling, and

$$\sin 2(\phi_1 - \phi_{p1}) = \frac{2}{\pi} r_1^* * \cos^2\theta_m * \{\beta * d(1 + \alpha * \sin^2\theta_m) - t_0 d\} \tag{9}$$

$$\sin 2(\phi_2 - \phi_{p2}) = \frac{2}{\pi} r_2^* * \cos^2\theta_m * \{\beta * d(1 + \alpha * \sin^2\theta_m) - t_0 d\} \tag{10}$$

$$r_i^* = \pi * k_{22}/(c_i^* * d)$$

for the twist coupling.

The right-hand sides depend on θ_m and β because the constants of integration are given in terms of these quantities.

Whereas the bulk equations depend on the equilibrium surface angles only, the boundary equations contain the preferential orientations θ_{pi} and ϕ_{pi} as well as the corresponding equilibrium values θ_i and ϕ_i. Therefore, we can decouple the system of non-linear equations to facilitate the mathematics. At first we solve the bulk equations in an iterative way (regula falsi) for a given set of surface angles θ_i and ϕ_i. Having found such a solution for η, β and λ, we use the boundary Equations (7)–(10) to calculate improved values of the equilibrium boundary angles. This procedure is repeated until stable solutions are found.

SPECIAL THEORY

For simplicity, we consider at first the case of asymmetric tilt coupling but symmetric and rigid twist coupling. Therefore, the total twist $\phi_0 = \phi_1 + \phi_2 = \phi_p$ is a constant.

A θ_m versus voltage curve with rigid tilt coupling but different preferential directions $\theta_{p1} = 5°$ and $\theta_{p2} = 10°$ is displayed in Figure 1. Qualitatively the curve (solid line) looks as in the case of symmetric coupling with the exception of the θ-values in the range $\theta_1 < \theta_m < \theta_2$. The solutions for θ_m in this region suffer from a peculiarity. The location of θ_m is outside of the sample. Within the sample $\theta(z)$ exhibits no extremum. This is not surprising if we look at Figure 2, where the corresponding tilt distributions are displayed for several values of the applied voltage. Because of the different pretilt angles at the boundaries there is a voltage region for which the director tilt varies monotonically throughout the sample. For lower and higher voltages θ_m is again located within the sample.

The curve (4) shows a nearly linear behaviour of the director tilt. The θ_m-branches corresponding to z-values outside of the sample are represented by the dashed lines in Figure 1. The assumption of θ_m to be located outside of the sample is interpreted as a mathematical trick to compute the director profiles. This is corroborated by the fact that the strange behavior of the θ_m-curve disappears, if we display the mid-plane tilt (dot-dashed line) instead of θ_m. We get a continuous line which for low and high values of θ coincides with the θ_m curve. In Figure 2 the boundary tilt angles do not vary with the voltage because we have assumed strong anchoring. The behaviour for weak anchoring is to be seen in Figure 4. In Figure 3 we have displayed the twist profiles

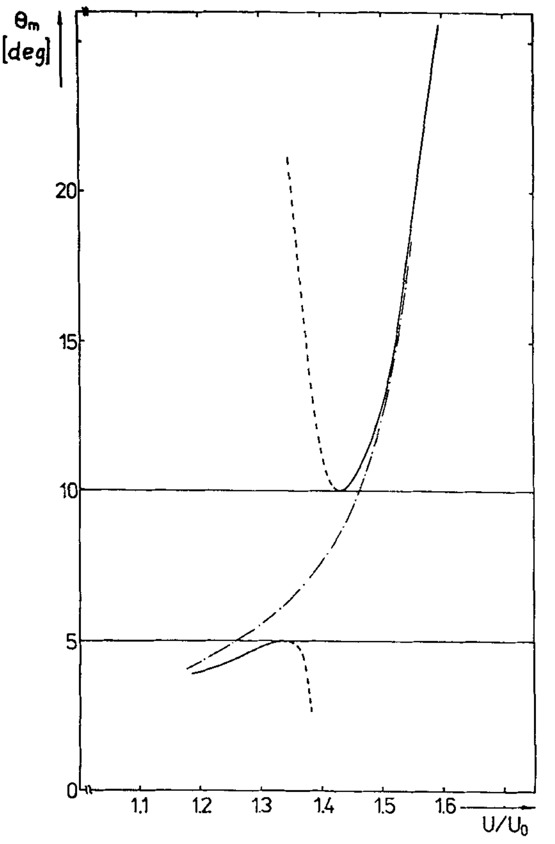

FIGURE 1 Director tilt versus applied voltage for a 180°-twisted layer with rigid tilt and twist coupling (solid —— line extreme director tilt θ_m, dot-dashed line -·-·-·- mid-plane tilt, dashed line ----- θ_m outside the sample). See text for material parameters.

corresponding to some voltage values of Figure 1. Distinct deviations from the homogeneous twist occur for high values of θ_m only.

Empirically, we found in the weak anchoring case the following relationship between the variations in the boundary tilt angles $(\theta_i - \theta_{pi})$ and the coupling constants c_i

$$c_1{*}(\theta_1 - \theta_{p1}) = c_2{*}(\theta_2 - \theta_{p2}). \tag{11}$$

We can derive this formula from Equation (7) and (8). Making a series expansion up to the 2. order in θ, we find for the right side

$$f(\theta) * w(\theta) = (a + b * \theta^2)^{1/2}$$

where a and b depend on η, λ and β and on the material parameters.

Therefore the right side is to a first approximation a constant and consequently Equation (11) is valid.

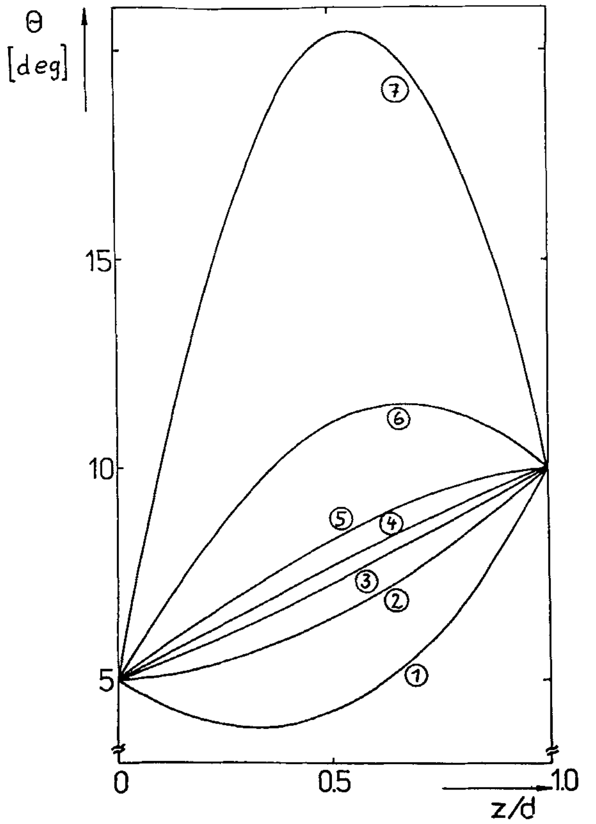

FIGURE 2 Tilt profiles of the layer of Figure 1 for different values of $u/u_0 = 1.21$ (1), 1.35 (2), 1.385 (3), 1.40 (4), 1.41 (5), 1.48 (6), 1.56 (7).

In the case of weak twist coupling we find a similar relation

$$\frac{c_1^*}{2} * \sin 2(\phi_1 - \phi_{p1}) = \frac{c_2^*}{2} * \sin 2(\phi_2 - \phi_{p2}). \tag{12}$$

For equal constants $c_1^* = c_2^*$ we get

$$\phi_1 - \phi_{p1} = \phi_2 - \phi_{p2}. \tag{13}$$

That means the variations of the twist angles at the boundaries are equal to each other and this equality holds even for asymmetrical tilt coupling.

RESULTS AND DISCUSSION

We choose the following material parameters in the computation of the director deformations

$$\alpha = 3.0, \quad \kappa = 1.0 \quad \text{and} \quad \gamma = 2.0$$

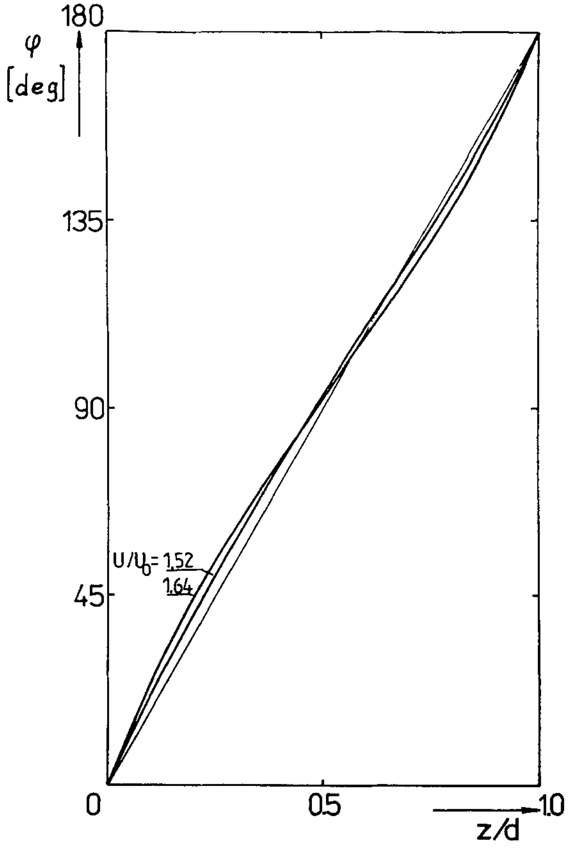

FIGURE 3 Twist profiles of the layer of Figure 1 for two different values of the reduced voltage.

if nothing otherwise is remarked. A chiral additive is given to the nematic host in such a quantity, that the resulting pitch corresponds with the twist induced by the boundary conditions. Voltages are expressed on a reduced scale, normalized by the threshold voltage u_0 of the planar Freedericksz cell.

In Figure 4 tilt profiles are displayed for a sample with quite different tilt coupling conditions at the boundaries (The twist coupling is strong in that case.). Depending on the applied voltage the equilibrium tilt at the right boundary can be greater or smaller, respectively, than that at the left boundary. The sample exhibits bistability in the range $1.53 < (u/u_0) < 1.84$. We remark that the equilibrium boundary tilts of the two lower branches deviate slightly from each other and from the pretilts.

In Figure 5 we display the tilt profiles for a 240°-twisted layer (rigid twist coupling) at different voltages. The pretilt at the left side is chosen to be zero. Therefore, minimum states cannot develop. For curve (3) the maximum θ_m coincides with the preferential boundary tilt on the right side. Surprisingly, by further lowering of the voltage the boundary tilt θ_2 increases again and becomes greater than the corresponding pretilt

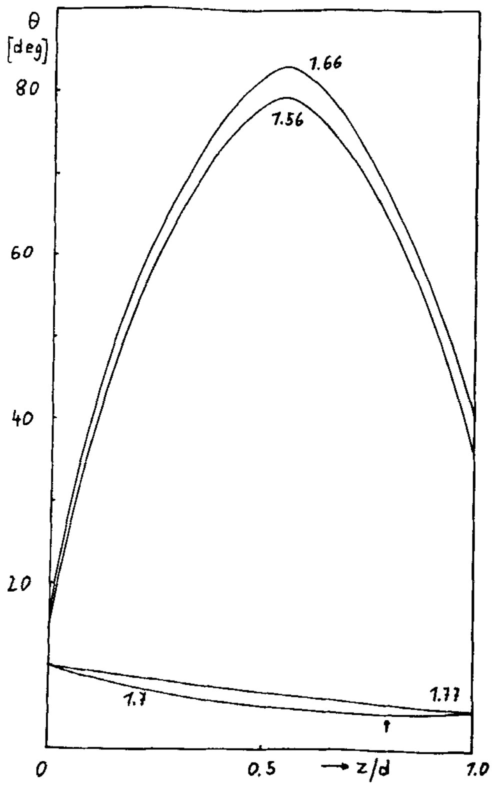

FIGURE 4 Tilt profiles of a 230°-layer with asymmetric tilt coupling $r_1 = 0.05, r_2 = 0.3, \theta_{p1} = 10°, \theta_{p2} = 5°$ and large bistability range for 4 values of the reduced voltage.

(curve 5). We do not believe in a numerical error because an enhancement of the numerical precision does not alter the result. We have not found such a behaviour for non-zero pretilts at both boundaries.

The deformation characteristic of a 240°-twisted layer is to be see in Figure 6 for different twist coupling constants. The tilt coupling is strong with a pretilt of $\theta_{p1} = \theta_{p2} = 10°$. In contrast to all other examples, here the helix parameter $t_0 d$ was chosen to be greater than the pretwist $\phi_p = 4.1888 < 4.6 = t_0 d$. In Figure 7 the corresponding twist and tilt profiles are displayed for different voltages. Because of the weak twist coupling the total twist varies with the applied voltage. The effective twist exceeds the pretwist for very low voltages because of the mismatch $\phi_p < t_0 d$. With increasing voltage the total twist becomes smaller, takes a minimum and again approaches the value of the pretwist.

There is a main difference between the tilt coupling and the twist coupling. The boundary tilt angles appear in the limits of integration of the bulk equations, but the boundary twist angles occur only in the total twist angle $\phi_0 = \phi_1 + \phi_2$ (see for Equation 4). Therefore one cannot distinguish between a variation in ϕ_1 and a variation in ϕ_2. Different twist coupling conditions at both boundaries do not change the

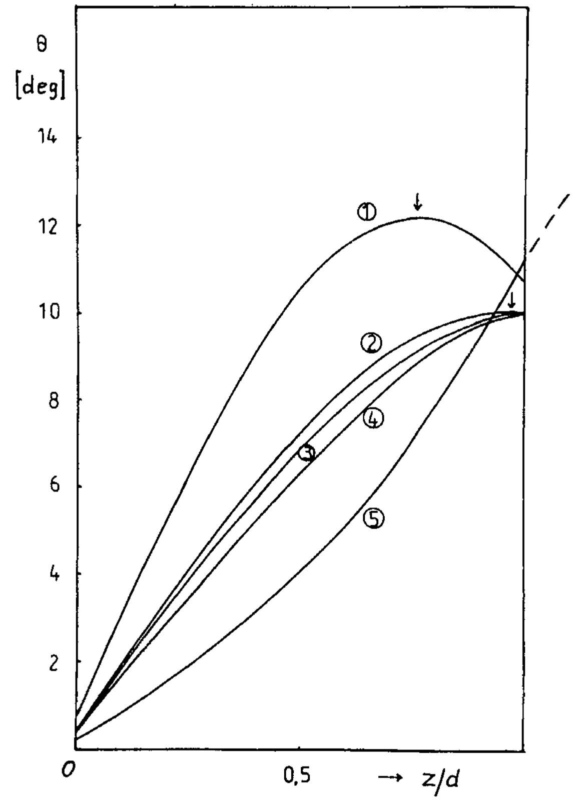

FIGURE 5 Tilt profiles of a 240°-twisted layer (rigid twist coupling) $r_1 = 0.1$, $r_2 = 0.2$, $\theta_{p1} = 0°$, $\theta_{p2} = 10°$ for 5 different values of $u/u_0 = 1.95$ (1), 1.922 (2), 1.915 (3), 1.90 (4), 1.70 (5).

symmetry of the tilt profile (see for Equations 7 and 8). The twist profile is calculated from a θ-integral. As long as $\theta_2 = \theta_1$ the twist profile always looks symmetrically with respect to the center of the sample.

On the other hand, it is sufficient to assume a weak twist coupling at one boundary and rigid twist coupling at the other one to describe all cases of interest without loss of generality.

PROBLEMS

The Rapini–Papoular ansatz suffers from some peculiarities. It determines only the orientation angles at the boundaries and has no influence on the tilt and twist profile within the sample. Therefore the Rapini–Papoular model simulates an interaction of zero range (contact interaction). Moreover, the applied model shows no interaction between the tilt and twist coupling. One can imagine that with increasing tilt angle the twist coupling becomes weaker.

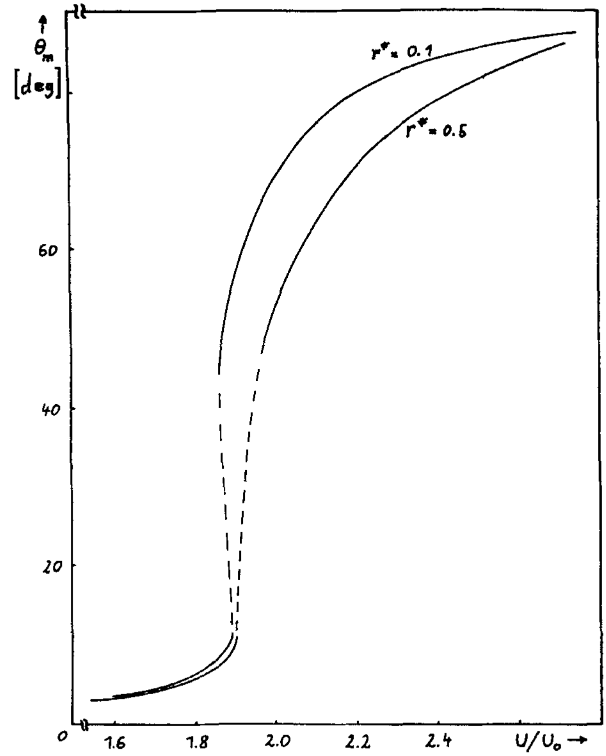

FIGURE 6 θ_m versus u/u_0 for a 240°-layer with strong tilt coupling for two values of the twist coupling constant r^*. The dashed lines are obtained by interpolation.

In the present paper we have not discussed the problem of the k_{13} and k_{24} contributions to the orientation. Both terms are called surface like elastic constants, since they come into play only for weakly anchored nematic layers. For planar distortions the saddle-splay term k_{24} is identically zero.[13] The k_{13} term may influence the values of the orientational angles at the boundary surfaces. But, the treatment of this term is still an object of controversy.[14,15,19] We have therefore neglected these boundary terms in our theory.

A last problem is the choice of the surface term itself. The term has to fulfill some physical basic requirements:

—existence of a preferential direction
—top-bottom symmetry of the molecules
—validity of HOOKs law for small deformations

One can construct a lot of surface terms which all fulfill the above requirements.[16] One example was given by HINOV.[17] But, up to now we have no possibility to find the interaction, which is most suited to model a given experimental situation.

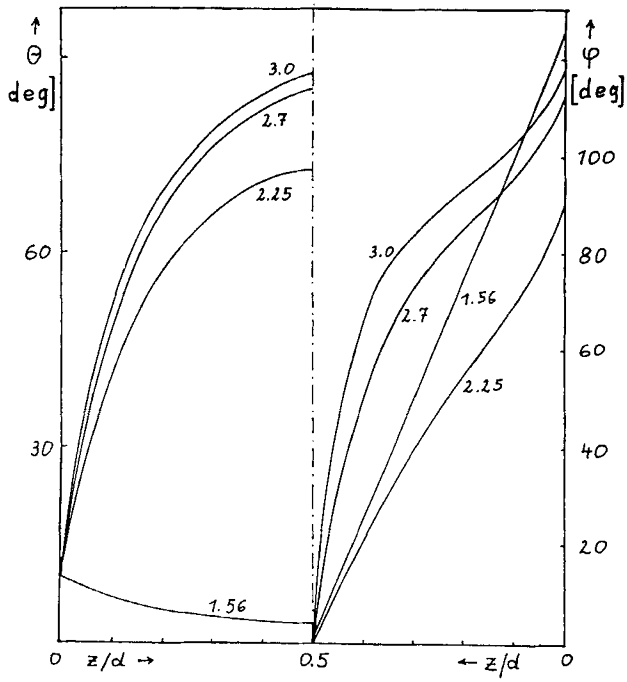

FIGURE 7 Tilt and twist profiles of the layer of Figure 6 with $r^* = 0.5$ for 4 different values of the reduced voltage.

References

1. J. Nehring, A. R. Kmetz and T. J. Scheffer, *J. Appl. Phys.*, **47**, 850 (1976).
2. H. A. van Sprang and P. A. Breddels, *J. Appl. Phys.*, **60**, 968 (1986).
3. R. Hirning, W. Funk, H.-R. Trebin, M. Schmidt and H. Schmiedel, *J. Appl. Phys.*,**70**, 4211 (1991).
4. D. W. Berreman, *Phil. Trans. R. Soc. Lond.*, **A309**, 203 (1983).
5. T. J. Scheffer and J. Nehring, *J. Appl. Phys.*, **58**, 3022 (1985).
6. J. Stelzer, R. Hirning and H.-R. Trebin, 22. Freiburger Arbeitstagung Flüssigkristalle, Freiburg, FRG, 1993, paper 24.
7. J. Congnard, *Mol. Cryst. Liq. Cryst. Suppl.*, **1**, 1 (1982).
8. B. Jerome, *Rep. Prog. Phys.*, **54**, 391 (1991).
9. W. L. Wagner, *Mol. Cryst. Liq. Cryst.*, **209**, 85 (1991).
10. Sin-Doo Lee and J. S. Patel, *Phys. Rev. Lett.*, **65**, 56 (1990).
11. A. Rapini and M. Papoular, *J. Phys. (Paris) Colloq.*, **30**, C4–54 (1969).
12. F. C. Frank, *Disc. Faraday Soc.*, **25**, 19 (1958).
13. G. Barbero and A. Strigazzi, *J. Phys., (Paris) Lett.*, **45**, L-857 (1984).
14. G. Barbero and C. Oldano, *Mol. Cryst. Liq. Cryst.*, **168**, 1 (1989).
15. H. P. Hinov, *Mol. Cryst. Liq. Cryst.*, **168**, 7 (1989).
16. B. Piesick, Dissertation 1978, Humboldt-Universität Berlin, unpublished
17. H. P. Hinov, *J. Phys. (Paris) Lett.*, **38**, L-215 (1977).
18. A. Strigazzi, *J. Phys. (Paris)*, **46**, 1507 (1985).
19. S. Žumer and S. Kralj, *Liq. Cryst.*, **12**, 613 (1992).